

## SUPPLEMENTARY MATERIAL

### MR-based cardiac and respiratory motion correction of PET: Application to static and dynamic cardiac $^{18}\text{F}$ -FDG imaging

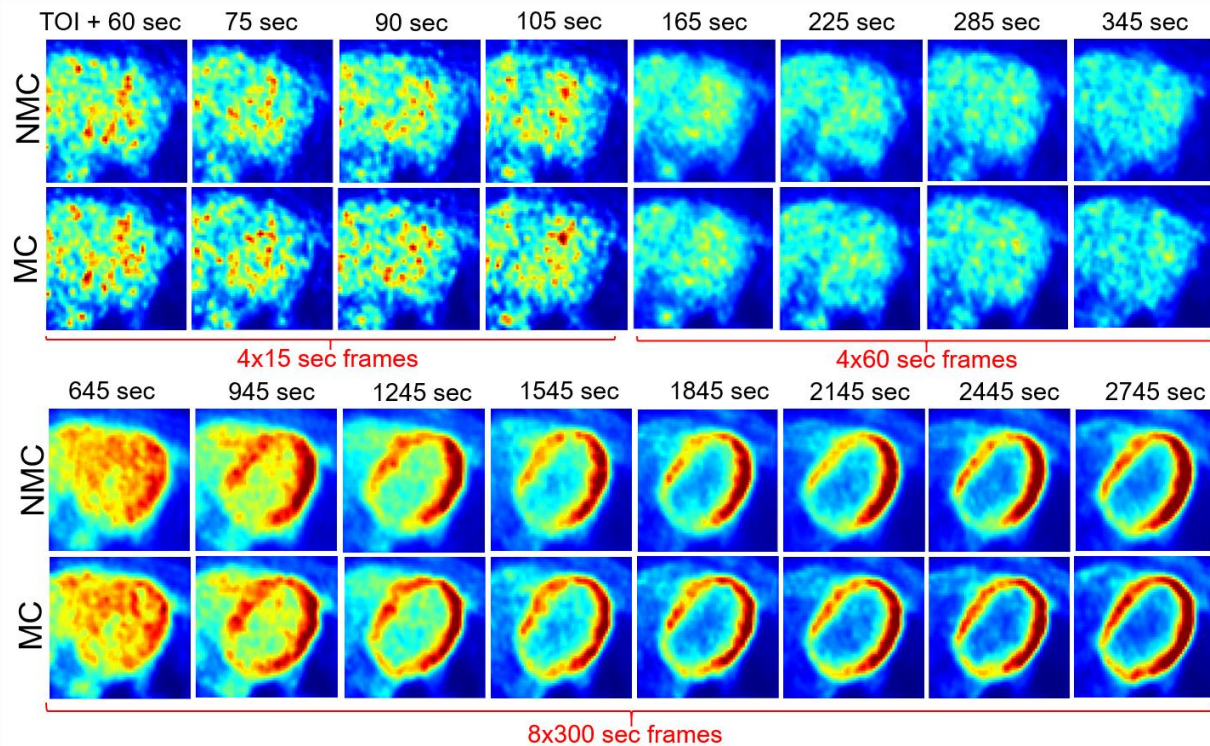
Y Petibon\*, T Sun\*, P K Han, C Ma, G El Fakhri and J Ouyang\*\*

Gordon Center for Medical Imaging, Department of Radiology, Massachusetts General Hospital and Harvard Medical School, Boston MA.

\* Equal contribution

\*\* Corresponding author: ouyang.jinsong@mgh.harvard.edu

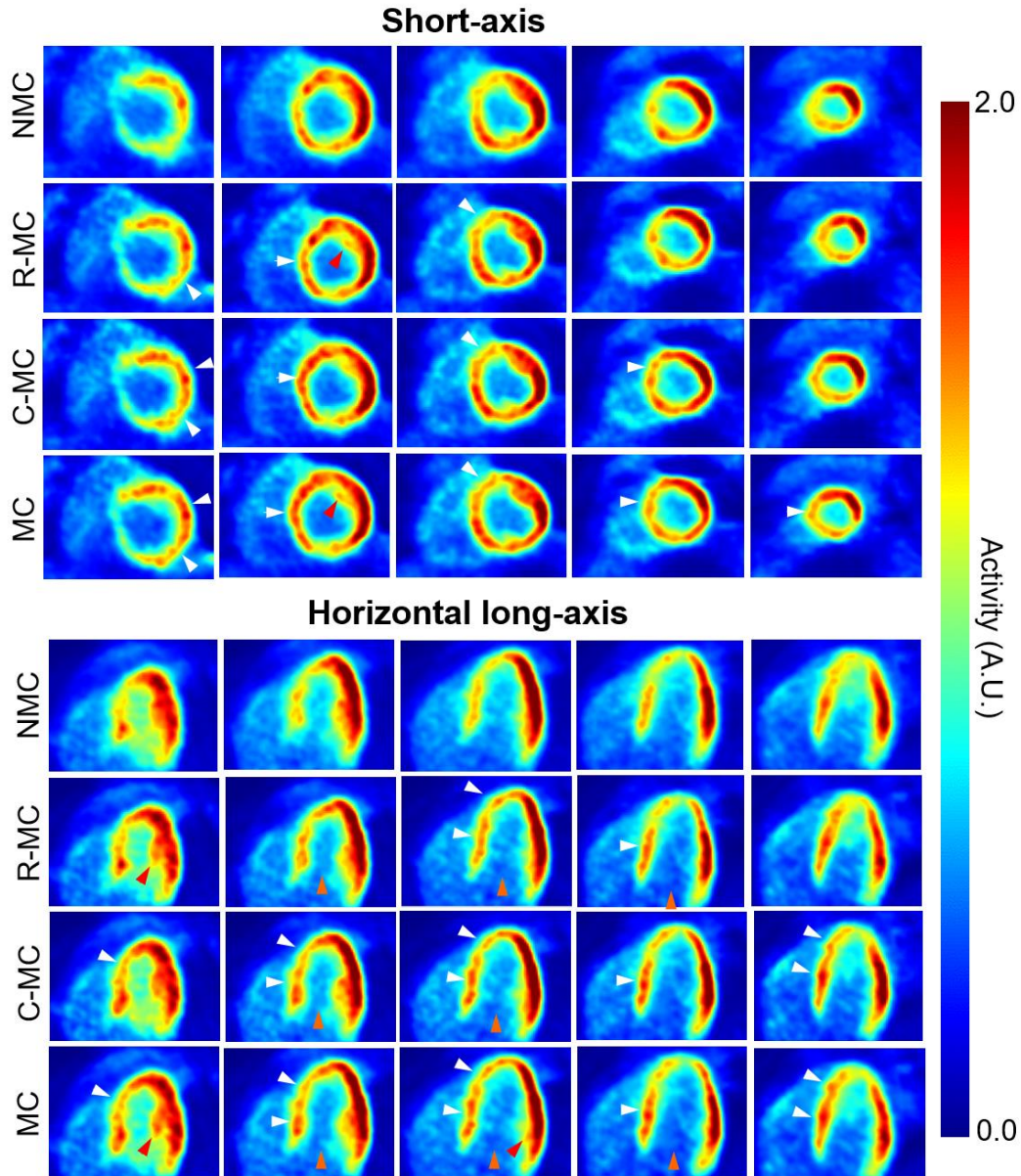
#### 1. Impact of motion correction across dynamic frames



**Supplemental Figure 1:** Same transverse slice across dynamic frames for NMC and MC methods (subject 1). Note that, to facilitate comparison of NMC and NMC images, the display range was adapted specifically for each dynamic frame. The first 4 frames after injection are not included in the figure as they were not corrected for motion. TOI = time of injection.

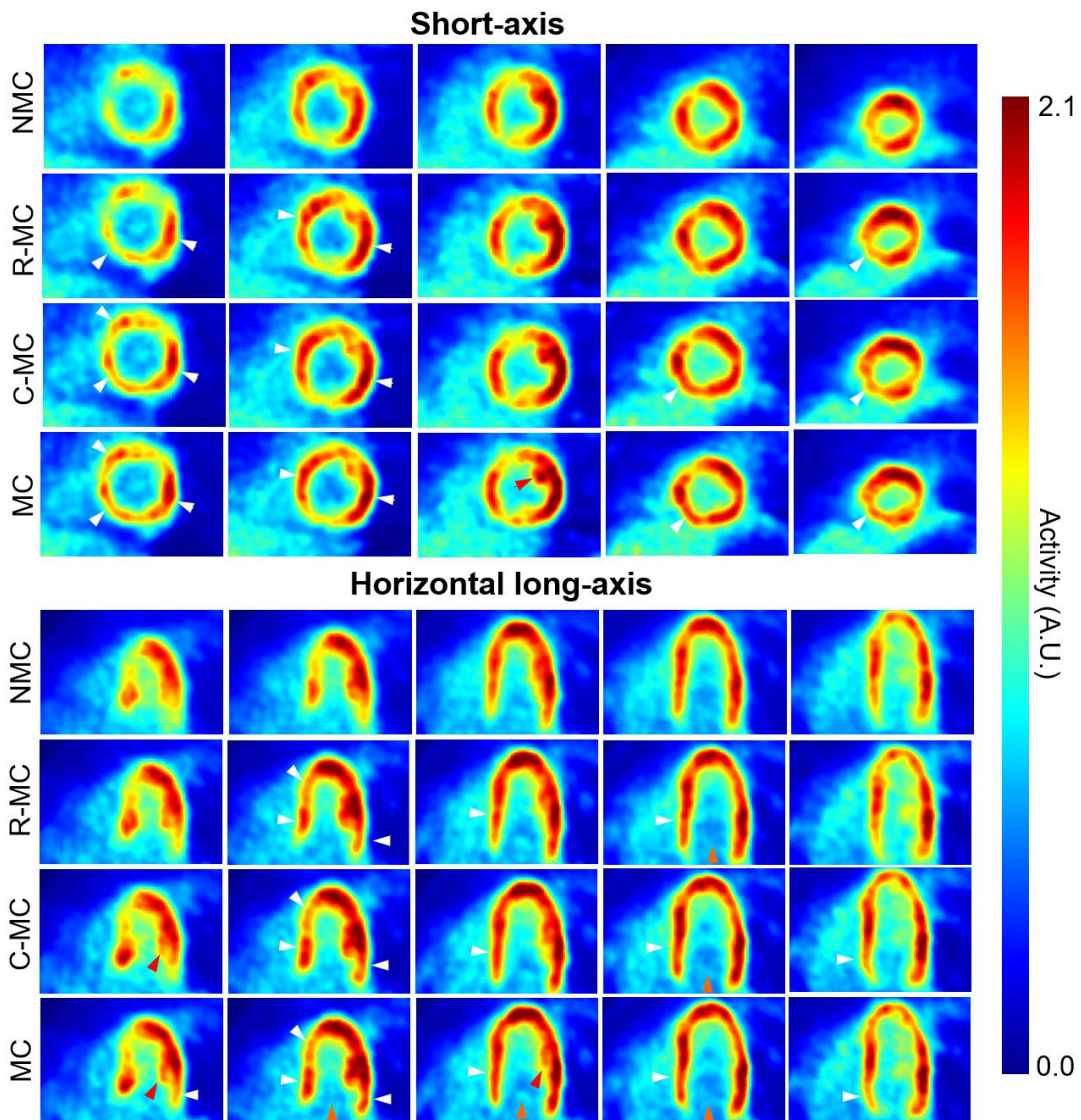
## **2. Relative impact of respiratory, cardiac and dual (i.e. respiratory + cardiac) motion correction**

To evaluate the relative impact of respiratory and cardiac motion correction, **Supplemental Figures 2-5** show images of activity and  $K_i$  obtained without motion correction ('NMC') and with respiratory-only (R-MC), cardiac-only (C-MC) and both respiratory and cardiac motion correction ('MC', as used throughout the article). Respiratory (respectively, cardiac) MC images were obtained by motion-compensated reconstruction (**Eq. 3**) of the respiratory- (cardiac-) gated sinograms using the motion fields determined with the golden-angle (tagging) MRI sequence.

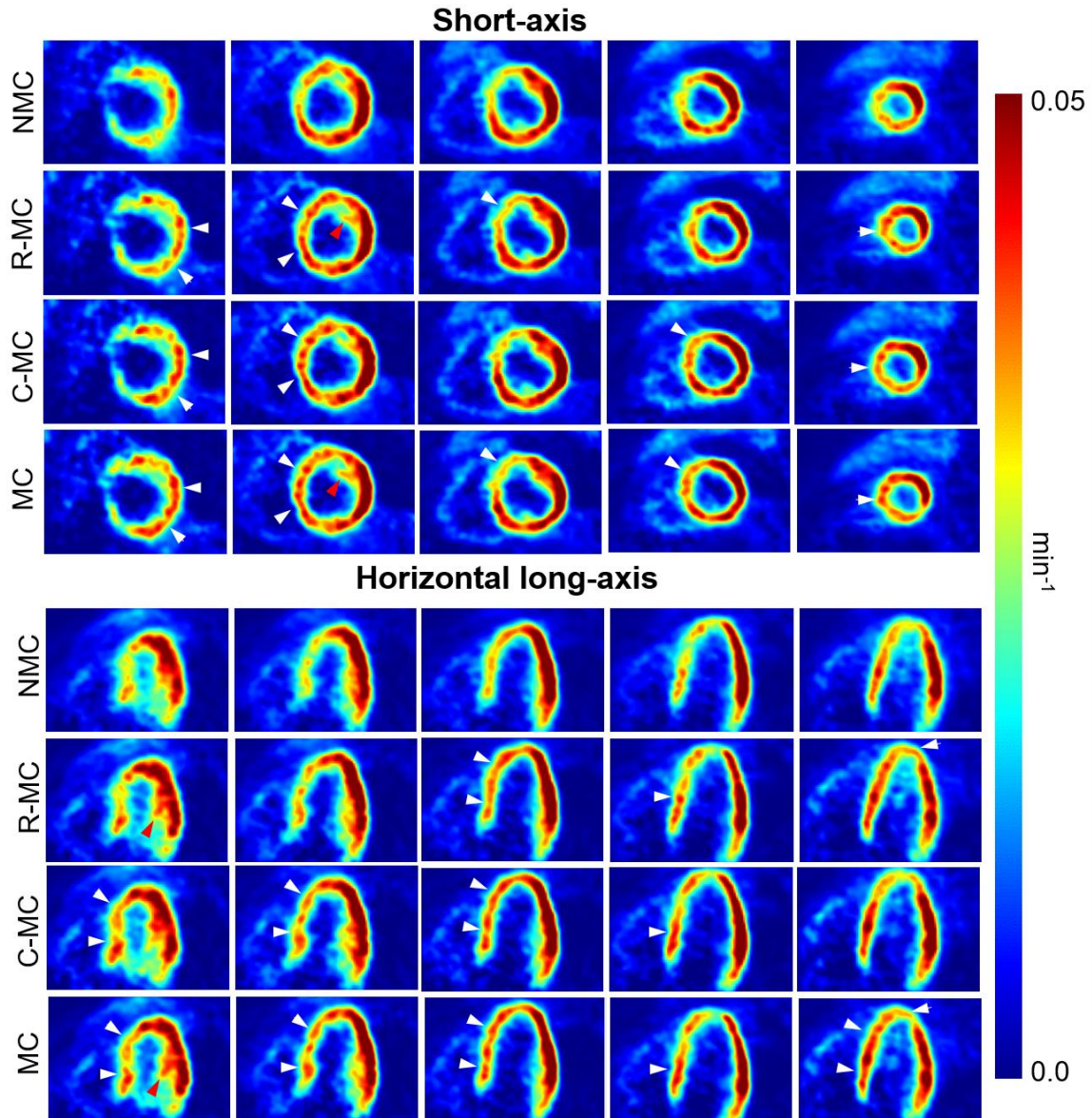


**Supplemental Figure 2:** Short-axis and horizontal long-axis images of a late dynamic frame reconstructed with NMC, respiratory MC ('R-MC'), cardiac MC ('C-MC') and both respiratory and cardiac MC ('MC') for subject 1. White arrows in motion corrected images indicate locations where the reconstructed wall activity is clearly higher than in NMC. Red arrows point to papillary muscles whose structure is more visible in corrected images, indicating improved spatial resolution. Orange arrows indicate areas where spillover from the myocardium to the left-

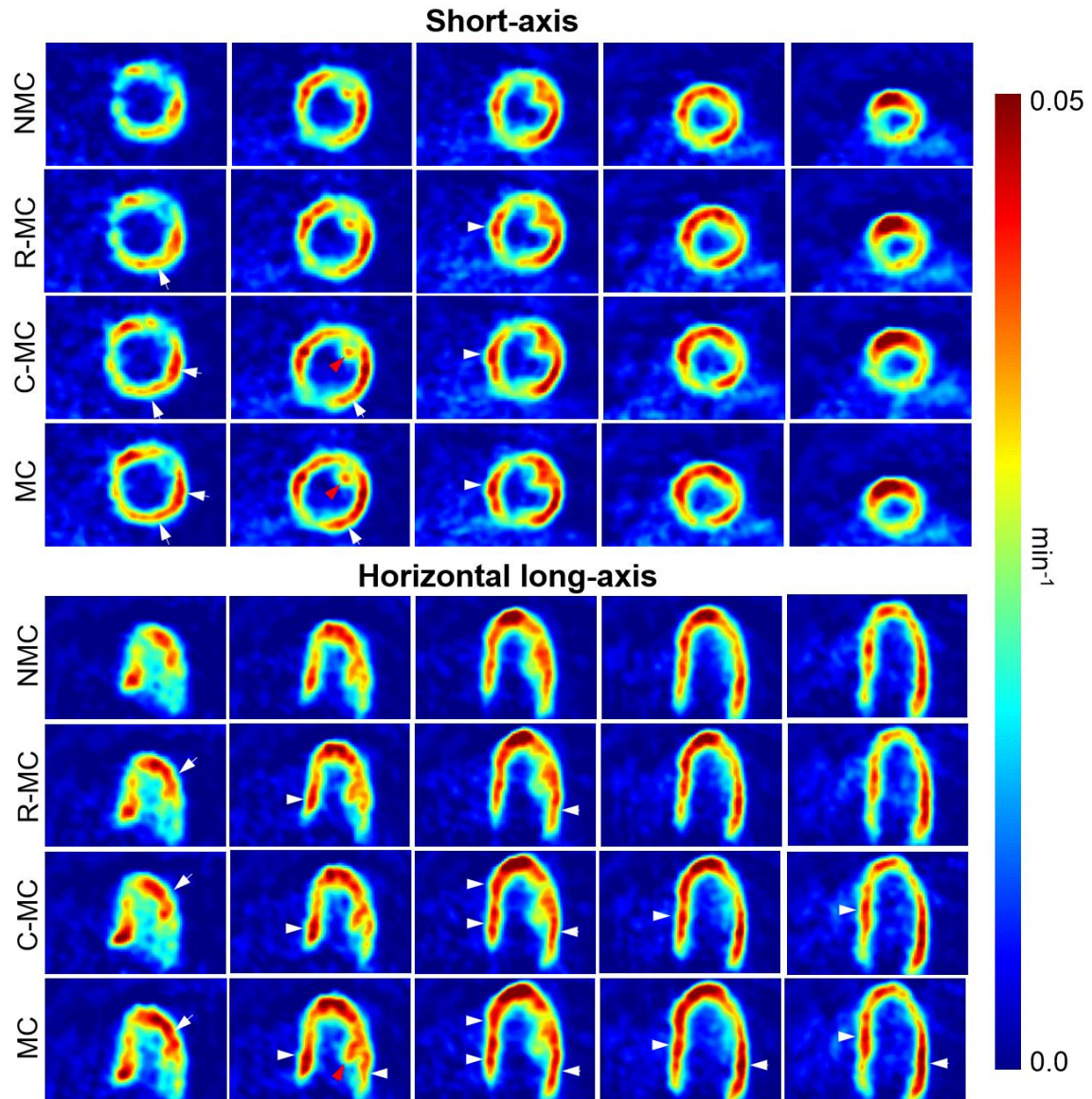
ventricle cavity is visibly reduced in motion corrected images.



**Supplemental Figure 3:** Short-axis and horizontal long-axis images of a late dynamic frame reconstructed with NMC, respiratory MC ('R-MC'), cardiac MC ('C-MC') and both respiratory and cardiac MC ('MC') for subject 2.



**Supplemental Figure 4:** Short-axis and horizontal long-axis  $K_i$  slices obtained using NMC, respiratory MC ('R-MC'), cardiac MC ('C-MC') and both respiratory and cardiac MC ('MC') for subject 1. Motion corrected images yielded overall higher  $K_i$  values than NMC, especially in regions evidenced by white arrows. Structures such as papillary muscles are also easier to delineate in motion corrected  $K_i$  maps (see red arrows).



**Supplemental Figure 5:** Short-axis and horizontal long-axis K<sub>i</sub> slices obtained using NMC, respiratory MC ('R-MC'), cardiac MC ('C-MC') and both respiratory and cardiac MC ('MC') for subject 2.